SCIENTIFIC REPORTS

Spin-helical Dirac states in graphene induced by polar-substrate surfaces with giant spin-orbit interaction: a new platform for spintronics

S. V. Eremeev[1,2,3], I. A. Nechaev[2,3], P. M. Echenique[3,4,5] & E. V. Chulkov[3,4,5]

[1]Institute of Strength Physics and Materials Science, 634021 Tomsk, Russia, [2]Tomsk State University, 634050 Tomsk, Russia, [3]Donostia International Physics Center (DIPC), 20018 San Sebastián/Donostia, Basque Country, Spain, [4]Departamento de Física de Materiales UPV/EHU, Facultad de Ciencias Químicas, UPV/EHU, Apdo. 1072, 20080 Sebastián/Donostia, Basque Country, Spain, [5]Centro de Física de Materiales CFM - MPC, Centro Mixto CSIC-UPV/EHU, 20080 San Sebastián/Donostia, Basque Country, Spain.

Spintronics, or spin electronics, is aimed at efficient control and manipulation of spin degrees of freedom in electron systems. To comply with demands of nowaday spintronics, the studies of electron systems hosting giant spin-orbit-split electron states have become one of the most important problems providing us with a basis for desirable spintronics devices. In construction of such devices, it is also tempting to involve graphene, which has attracted great attention because of its unique and remarkable electronic properties and was recognized as a viable replacement for silicon in electronics. In this case, a challenging goal is to lift spin degeneracy of graphene Dirac states. Here, we propose a novel pathway to achieve this goal by means of coupling of graphene and polar-substrate surface states with giant Rashba-type spin-splitting. We theoretically demonstrate it by constructing the graphene@BiTeCl system, which appears to possess spin-helical graphene Dirac states caused by the strong interaction of Dirac and Rashba electrons. We anticipate that our findings will stimulate rapid growth in theoretical and experimental investigations of graphene Dirac states with real spin-momentum locking, which can revolutionize the graphene spintronics and become a reliable base for prospective spintronics applications.

Graphene is a fascinating material, which has attracted great attention because of its unique electronic properties[1,2]. In graphene spintronics, many efforts were made to realize a robust control of electron spins by, e.g., magnetoelectric coupling or spin-orbit interaction (SOI)[3–5]. Main hopes were pinned on the SOI effect, which can be directly observed[6,7].

Some interesting phenomena, such as quantum spin Hall effect[8], quantum anomalous Hall effect[9], and other phenomena were predicted in graphene. However, the intrinsic spin-orbit splitting in pristine graphene is proved to be too weak for producing an observable effect and for realizing practical applications[8,10,11]. The major challenge in graphene spintronics thus is to lift spin degeneracy of the graphene Dirac states, which makes them spin-polarized with some spin texture similar to that, e.g., in topological insulators (TIs). In principle, it can be realized by applying an extrinsic SOI, i.e., by placing the grapnene in a proper medium with a strong spin-orbit coupling. Numerous previous works, both experimental and theoretical, have been aimed at enhancement of graphene SOI via, e.g., adatoms deposition[9,12–14] or growth of graphene on metal substrates[15–19].

Recently, it was shown that the Te-terminated surface of non-centrosymmetric hexagonal-structured polar-semiconductor compounds BiTeX (with X = Cl,Br,I) meet requirements for spintronics applications, since these systems hold a giant Rashba spin splitting of a free-electron-like surface state at the $\bar{\Gamma}$ point[20–25]. The mentioned bismuth tellurohalides are characterized by ionic bonding with large charge transfer from bismuth to halide- and tellurium-atomic layers. The spin-split surface states at the Te-terminated surface emerge by splitting off from the lowest conduction band, owing to the decreasing potential within the near-surface layers[20], which is a consequence of strong ionicity. One can expect that deposition of graphene on BiTeX, can result in a strong interaction and hybridization of the Rashba and Dirac two-dimensional (2D) electrons. In designing such systems, it is important to match the lattice parameters of the contacting materials. The in-plane hexagonal

parameter of BiTeCl matches perfectly with the parameter of $\sqrt{3} \times \sqrt{3}$ graphene. Thus, the deposited graphene should not undergo the in-plane strain [Fig. 1(a)]. In the $\sqrt{3} \times \sqrt{3}$ structure, the Brillouin zone of graphene takes a third of the original one [Fig. 1(b)]. Under this folding, the $\bar{K}$-point Dirac cone of graphene appears as the four-fold degenerate $\bar{\Gamma}$ state [Fig. 1(c)] with linear dispersion in the vicinity of the Dirac point (Fig. 1(c), the dotted-line rectangle). Thus, both the Dirac state and the Rashba state of the pristine substrate [Fig. 1(d)] reside in the Brillouin zone center.

The interaction of the two 2D electron systems results in a strong modification of the spectra with respect to the constituents (Fig. 2). In the upper part of the gap, at large $k_{||}$ the Rashba state of BiTeCl preserves its original shape, while at $k_{||} \lesssim 0.1$ Å^{-1} both inner and outer branches of the Rashba state rapidly become strongly hybridized with graphene cone states. Already at $k_{||} \approx 0.05$ Å^{-1} they start to turn into the grephene-derived states completely localized within the graphene layer and dispersing towards the Dirac point immersed in the conduction band of the substrate bulk states. In the lower part of the gap, approaching the $\bar{\Gamma}$ point two of four graphene bands start to hybridize with the substrate surface state forming a hole-like Rashba state near the valence band, which is completely localized within substrate uppermost layers in the vicinity of the $\bar{\Gamma}$ point. Thus, at small $k_{||}$ the hybridization of two of four graphene branches with

Figure 2 | Electronic structure of graphene@BiTeCl. Band structure of BiTeCl (0001) slab with $\sqrt{3} \times \sqrt{3}$ graphene on Te-terminated surface. Red and blue circles denote weights of the states localized in the outermost three layers (1-st TL) of BiTeCl and in graphene layer, respectively. Shaded by green color regions indicate projected bulk bands of substrate.
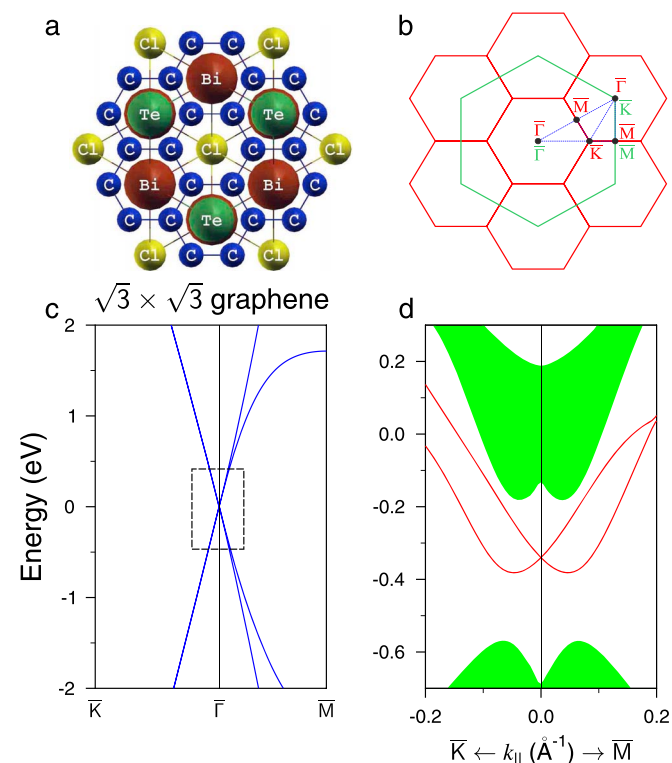

Figure 1 | Atomic structure of graphene on BiTeCl and electronic spectra of the pristine graphene and Te-terminated BiTeCl surface. (a) Top view for the $\sqrt{3} \times \sqrt{3}$ graphene on the Te-terminated surface of BiTeCl. Carbon atoms are shown by dark blue balls; green, maroon, and yellow balls denote first-layer Te atom, second-layer Bi atom, and third-layer Cl atom, respectively; (b) Scheme of $\sqrt{3} \times \sqrt{3}$ folding of the 2D BZ of graphene: green and red colors correspond to the 1×1 and $\sqrt{3} \times \sqrt{3}$ BZs, respectively; (c) Band structure of the $\sqrt{3} \times \sqrt{3}$ graphene (dashed rectangle marks the $E(k)$ region in the vicinity of the $\bar{\Gamma}$ point, where all graphene bands have the linear dispersion); (d) Electronic spectrum of the Te-terminated BiTeCl surface. The Rashba-split surface state is shown by red line, projected bulk band structure is depicted by green areas.
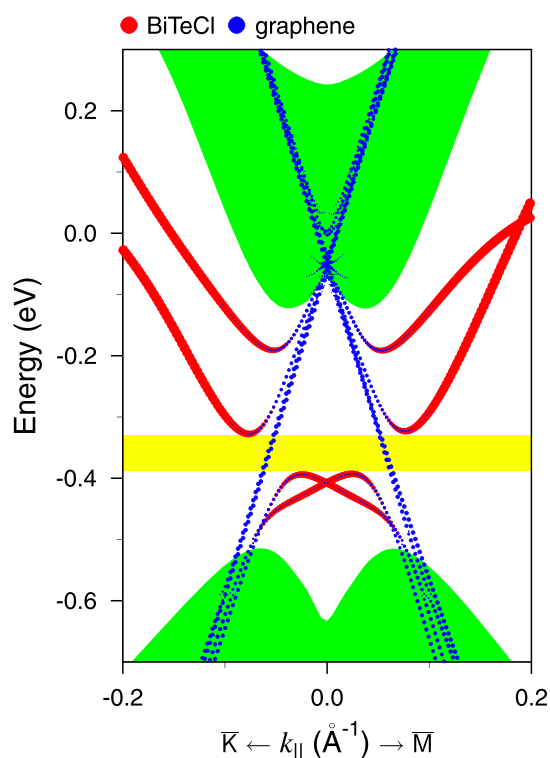
the Rashba state of the BiTeCl substrate leads to a break of both branches of the Rashba state in such a way that its degeneracy point appears near the valence band or, to the contrary, the Rashba states break two graphene bands. Other two Dirac bands remain unchanged and are localized in the graphene layer for all $k_{||}$. As a result of these changes, in the middle part of the bulk band gap, within the energy interval of 70 meV (see yellow stripe in Fig. 2), two almost degenerate Dirac states of graphene survive. The small SOI-induced $k_{||}$-splitting for the Dirac cones is less then 0.002 Å^{-1}.

The spin structure of the surface states within the $\bar{\Gamma}$ band gap is shown in Fig. 3(a). As seen in the figure, at large $k_{||}$ the Rashba branches preserve the spin polarization of the clean Te-terminated BiTeCl surface: they demonstrate the counter-clockwise and clockwise in-plane helicity for the inner and outer branch, respectively. At $k_{||} < 0.1$ Å^{-1}, where due to hybridization the Rashba branches turn into the Dirac states and start to be localized at the graphene layer, the spin helicity of the graphene band hybridizing with the outer branch becomes the same as that of the inner branch. Consequently, both hybridized graphene bands have the counter-clockwise spin polarization. The two remaining non-hybridized Dirac bands are characterized by the clockwise spin polarization, as clearly seen in Fig. 3(a). Thus, and this is the main issue of the present study, the hybridization between the graphene and substrate-Rashba-split 2D electrons provides the helical spin separation of the graphene Dirac states.

As was mentioned above, the most interesting feature of the graphene@BiTeCl spectrum is the energy window of 70 meV width, where the Dirac states of graphene exist only (see yellow stripe in Fig. 2). The two almost degenerate Dirac states have the same in-plane spin polarization, which can be clearly seen in Fig. 3(b), where spin-resolved constant energy contours in the middle of this energy
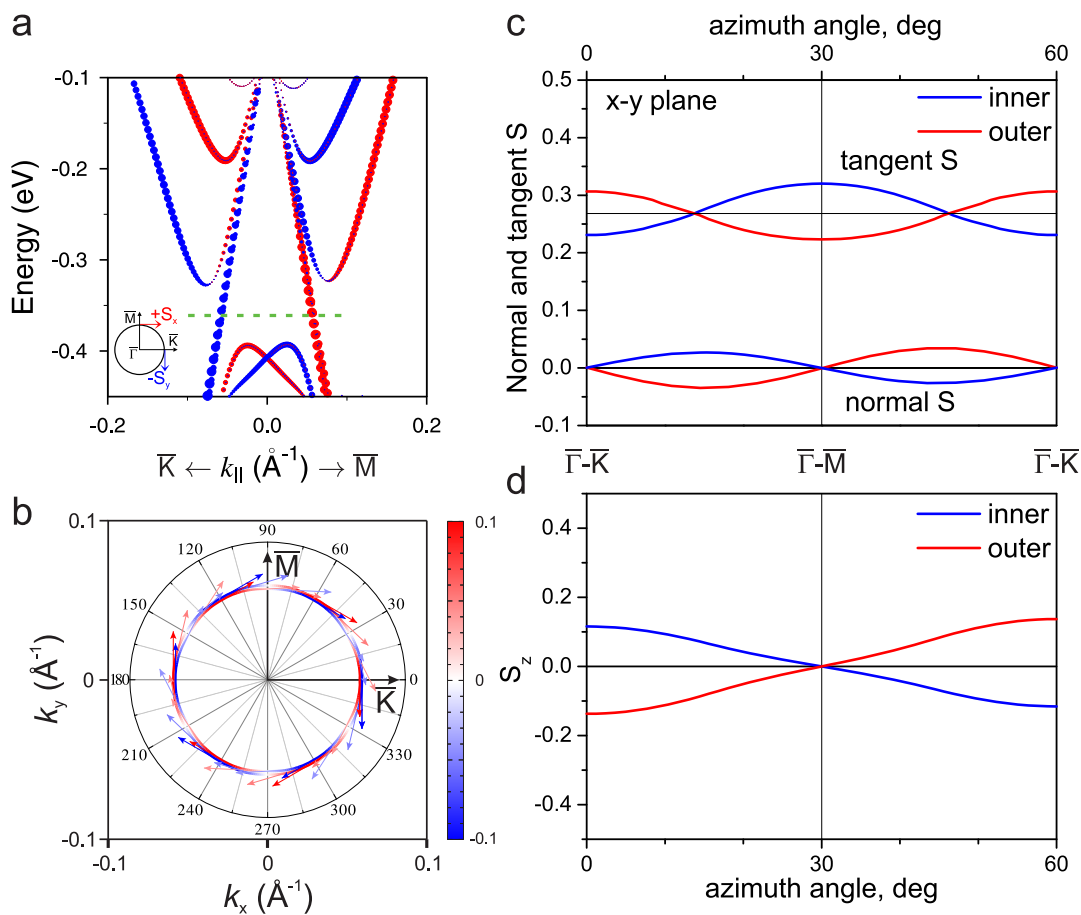
2

Figure 3 | Spin structure of the surface states. (a) The spin-resolved electronic spectrum of the surface states where the filled circles represent the value of the in-plane spin component (red and blue colors denote positive and negative values of spin, respectively, for mutually perpendicular $\bar{\Gamma}-\bar{M}$ and $\bar{\Gamma}-\bar{K}$ directions as schematically shown in inset); (b) Constant energy contours for graphene Dirac-cone bands at energy of -365 meV, marked by dashed green line in panel (a). Arrows adjacent to the contours denote the in-plane spin component. The out-of-plane spin component is indicated by the colour with red and blue corresponding to the upward and downward directions, respectively; Azimuthal dependencies of the graphene spin components, including the in-plane components in the tangent and normal directions to the contours (c) and out-of-plane component (d), inner and outer Dirac contours shown by blue and red, respectively.

window are shown. Both Dirac states, apart from the in-plane clockwise spin polarization, also demonstrate the presence of the out-of-plane spin component, which is intrinsic feature of the spin-polarized states at hexagonal surfaces. The detailed spin texture is illustrated in Figs. 3(c) and (d). Fig. 3(c) shows the azimuthal dependencies of the in-plane spin components in the tangent and normal directions to the inner and outer Dirac contours. One can see that the tangent component for both bands demonstrates variation around the value of 0.27, while the normal component experiences small variations near zero spin value. For both bands, the out-of-plane spin component S_z [Fig. 3(d)] also varies near zero but the variations are significantly larger than those for the normal component. Nevertheless, the maximal out-of-plane spin values, which are observed along the $\bar{\Gamma}-\bar{K}$ directions, are three times smaller than the magnitude of the tangent in-plane spin component. Furthermore, the signs of both normal and out-of-plane spin components are opposite for the inner and outer almost degenerate Dirac contours, what results in a fully helical net in-plane spin polarization of the Dirac electrons.

Apparently, the revealed possibility to create the helical spin-polarized Dirac electrons in graphene opens up new horizons in the graphene-based spintronics. The mentioned spin texture of the graphene Dirac states is important to come out as a consequence of the strong hybridization between graphene and giant Rashba-split states of the Te-terminated surface of the polar substrate

BiTeCl. Due to excellent matching of lattice parameters of BiTeCl and graphene, the graphene@BiTeCl system can be easily realized in practice. The reported energy interval of $\sim$70 meV in the middle part of the projected bulk energy gap, where the spin-polarized Dirac states solely exist, is sufficiently enough for spintronics applications. However, it should be noted that this energy interval in the real system can differ from the density functional theory (DFT) prediction. As shown both by experiment[24] and by the *GW* bulk calculations[26], the bulk band gap in BiTeCl is a factor of two larger than that predicted by DFT. Besides, *GW* bulk calculations modify the Rashba parameters of the bulk bands too, bringing them close to the experimental values. In turn, it can affect the Rashba splitting of the surface state, resulting in modification of the Dirac/Rashba hybridization and, consequently, altering the hybridization gap in the Rashba state. In order to actively bring the spin-polarized Dirac states located in the middle part of the gap into play, the chemical potential of the system should be decreased by $\sim$350 meV with respect to the Fermi level obtained in the present calculation. The chemical potential tuning can be realized by applying an external electric field or by doping with hole-donating adsorbates. The latter approach seems to be preferable. As was recently shown for Au/Si system, supporting Rashba-split surface state, the Fermi level position can be effectively tuned within the range of $\sim$350 meV by choosing appropriate adsorbate species[27].

In the context of spintronics applications, the revealed remarkable features of graphene@BiTeCl indicate that the well-defined carrier spin separation can be introduced into graphene-based devices by using polar semiconductor substrates with strong SOI. Moreover, graphene@BiTeCl can come up to take the place of topological insulators in a rich variety of devices utilizing spin-polarized transport, which were suggested to exploit the spin-helical surface states in TIs and can make these devices more efficient. Actually, in both cases (graphene@BiTeCl and TI, like Bi_2Se_3) owing to p-type doping one can get the 2D states residing in the projected bulk band gap and protected from backscattering by helical in-plane spin polarization. However, graphene@BiTeCl has quite a few advantages over the TI: the significantly higher Fermi velocity, the larger number of spin carriers, the essentially stronger localization of the states (the single atomic layer of graphene versus five or seven atomic layers in TIs), and the notably weaker dielectric screening of the Coulomb interaction between 2D electrons caused by surrounding medium (the dielectric constant $\varepsilon_{medium} \sim 10$ versus ~ 25–100 in TIs).

Except the spin-polarized Dirac states in the middle part of the gap, the surface states in upper and lower parts of the bulk gap may also be of considerable interest, because in the respective energy regions the helical Dirac states of graphene and Rashba spin-split states coexists. Various intriguing physical phenomena related to decay of elementary excitations in the states with different velocities can be expected.

Methods

Our calculations were based on the DFT as implemented in the Vienna *ab initio* simulation package VASP[28]. The generalized gradient approximation (GGA) of Perdew, Burke, and Ernzerhof (PBE) to the exchange-correlation (XC) potential has been used. The interaction between the ion cores and valence electrons was described by the projector augmented-wave method[29]. Relativistic effects, including spin-orbit coupling, were fully taken into account. To simulate BiTeCl substrate we consider a 24 atomic layer slab. Hydrogen monolayer was used to passivate the chlorine side of the slab as was described in Ref. 20. The positions of atoms in the graphene layer and in three outermost atomic layers of the BiTeCl slab (both along the z axis normal to the surface and within the xy plane) were optimized including SOI self-consistently. The equilibrium structure of graphene@BiTeCl, where C-honey-combs are centered with surface Te atoms, subsurface Bi atoms, and third-layer Cl atoms (see Fig. 1(a)), has the graphene layer that lies ≈ 3.35 Å above the substrate surface layer. The atoms of the deeper layers were kept fixed at the bulk crystalline positions. The k-point mesh of $9 \times 9 \times 1$ was used for the Brillouin zone of the surface unit cell.

1. Geim, A. K. & Novoselov, K. S. The rise of graphene. *Nature Mater.* **6**, 183 (2007).
2. Castro Neto, A. H., Guinea, F., Peres, N. M. R., Novoselov, K. S. & Geim, A. K. The electronic properties of graphene. *Rev. Mod. Phys.* **81**, 109 (2009).
3. Žutić, I., Fabian, J. & Das Sarma, S. Spintronics: Fundamentals and applications. *Rev. Mod. Phys.* **76**, 323 (2004).
4. Awschalom, D. D. & Flatte, M. E. Challenges for semiconductor spintronics. *Nature Phys.* **3**, 153 (2007).
5. Zhang, Z., Chen, C., Guo, W. Magnetoelectric Effect in Graphene Nanoribbons on Substrates via Electric Bias Control of Exchange Splitting. *Phys. Rev. Lett.* **103**, 187204 (2009).
6. Kato, Y. K., Myers, R. C., Gossard, A. C. & Awschalom, D. D. Observation of the Spin Hall Effect in Semiconductors. *Science* **306**, 1910 (2004).
7. Wunderlich, J., Kaestner, B., Sinova, J. & Jungwirth, T. Experimental Observation of the Spin-Hall Effect in a Two-Dimensional Spin-Orbit Coupled Semiconductor System. *Phys. Rev. Lett.* **94**, 047204 (2005).
8. Kane, C. L. & Mele, E. J. Quantum Spin Hall Effect in Graphene. *Phys. Rev. Lett.* **95**, 226801 (2005).
9. Qiao, Z. et al. Quantum anomalous Hall effect in graphene from Rashba and exchange effects. *Phys. Rev. B* **82**, 161414 (2010).
10. Yao, Y., Ye, F., Qi, X.-L., Zhang, S.-C. & Fang, Z. Spin-orbit gap of graphene: First-principles calculations. *Phys. Rev. B* **75**, 041401 (2007).
11. Gmitra, M., Konschuh, S., Ertler, C., Ambrosch-Draxl, C. & Fabian, J. Band-structure topologies of graphene: Spin-orbit coupling effects from first principles. *Phys. Rev. B* **80**, 235431 (2009).
12. Castro Neto, A. H. & Guinea, F. Impurity-Induced Spin-Orbit Coupling in Graphene. *Phys. Rev. Lett.* **103**, 026804 (2009).
13. Abdelouahed, S., Ernst, A., Henk, J., Maznichenko, I. V. & Mertig, I. Spin-split electronic states in graphene: Effects due to lattice deformation, Rashba effect, and adatoms by first principles. *Phys. Rev. B* **82**, 125424 (2010).
14. Weeks, C., Hu, J., Alicea, J., Franz, M. & Wu, R. Engineering a Robust Quantum Spin Hall State in Graphene via Adatom Deposition. *Phys. Rev. X* **1**, 021001 (2011).
15. Dedkov, Y. S., Fonin, M., Rüdiger, U. & Laubschat, C. Rashba Effect in the Graphene/Ni(111) System. *Phys. Rev. Lett.* **100**, 107602 (2008).
16. Varykhalov, A. et al. Electronic and Magnetic Properties of Quasifreestanding Graphene on Ni. *Phys. Rev. Lett.* **101**, 157601 (2008).
17. de Heer, W. A. et al. Epitaxial graphene electronic structure and transport. *J. Phys. D: Appl. Phys.* **43**, 374007 (2010).
18. Li, Z. Y., Yang, Z. Q., Qiao, S., Hu, J. & Wu, R. Q. Spinorbit splitting in graphene on metallic substrates. *J. Phys.: Condens. Matter* **23**, 225502 (2011).
19. Marchenko, D. et al. Giant Rashba splitting in graphene due to hybridization with gold. *Nature Commun.* **3**, 1232 (2012).
20. Eremeev, S. V., Nechaev, A. I., Koroteev, Y. M., Echenique, P. M. & Chulkov, E. V. Ideal Two-Dimensional Electron Systems with a Giant Rashba-Type Spin Splitting in Real Materials: Surfaces of Bismuth Tellurohalides. *Phys. Rev. Lett.* **108**, 246802 (2012).
21. Crepaldi, A. et al. Giant Ambipolar Rashba Effect in the Semiconductor BiTeI. *Phys. Rev. Lett.* **109**, 096803 (2012).
22. Landolt, G. et al. Bulk and surface Rashba splitting in single termination BiTeCl. *Phys. Rev. Lett.* **109**, 116403 (2012).
23. Eremeev, S. V., Nechaev, A. I. & Chulkov, E. V. Giant Rashba-type spin splitting at polar surfaces of BiTeI. *JETP Lett.* **96**, 437 (2012).
24. Sakano, M. et al. Strongly Spin-Orbit Coupled Two-Dimensional Electron Gas Emerging near the Surface of Polar Semiconductors. *Phys. Rev. Lett.* **110**, 107204 (2013).
25. Eremeev, S. V., Rusinov, I. P., Nechaev, A. I. & Chulkov, E. V. Rashba split surface states in BiTeBr. *New J. Phys.* **15**, 075015 (2013).
26. Rusinov, I. P. et al. Many-body effects on the Rashba-type spin splitting in bulk bismuth tellurohalides. *Phys. Rev. B* **87**, 205103 (2013).
27. Bondarenko, L. V. et al. Large spin splitting of metallic surface-state bands at adsorbate-modified gold/silicon surfaces. *Sci. Rep.* **3**, 1826 (2013).
28. Kresse, G. & Furthmüller, J. Efficiency of ab-initio total energy calculations for metals and semiconductors using a plane-wave basis set. *Comput. Mater. Sci.* **6**, 15-50 (1996).
29. Kresse, G. & Joubert, D. From ultrasoft pseudopotentials to the projector augmented-wave method. *Phys. Rev. B* **59**, 1758 (1999).

Acknowledgments

Author Contributions

S.V.E. carried out the theoretical calculation and prepared figures. S.V.E., I.A.N., P.M.E. and E.V.C. contrived the system, analyzed the data, and contributed to the discussion and writing the manuscript.

Additional information

Competing financial interests: The authors declare no competing financial interests.

How to cite this article: Eremeev, S.V., Nechaev, I.A., Echenique, P.M. & Chulkov, E.V. Spin-helical Dirac states in graphene induced by polar-substrate surfaces with giant spin-orbit interaction: a new platform for spintronics. *Sci. Rep.* **4**, 6900; DOI:10.1038/srep06900 (2014).